

The Origin of Large Cosmic-Ray Bursts

R. E. LAPP

Ryerson Physical Laboratory, University of Chicago, Chicago, Illinois

(Received November 30, 1945)

Integral size-frequency distribution curves for cosmic-ray bursts of more than 100 particles were obtained by using an ionization chamber shielded by 1.25, 12, and 35 cm of iron. These distribution curves can all be represented by an inverse power law with exponent $= 2.0 \pm 0.2$. The transition curve plotted from these data shows a pronounced maximum. Five G-M counter coincidence sets were arranged to register on the ionization chamber trace so that coincidences between bursts and air showers could be measured. For a thickness of 1.25 cm of iron, about 85 percent of the bursts were coincident with air showers, while for 12 cm of iron, this fraction was about 20 percent and for 35 cm of iron, only 5 percent of the bursts were observed to be coincident with extensive showers. A discussion is given to account for the origin of the bursts which were not coincident with air showers. For the analysis of the transition curve three different types of bursts are considered: bursts due to extensive atmospheric showers, bursts produced by narrow air showers or single high energy electrons, and bursts produced by mesotrons (knock-on and bremsstrahlung processes). Data for bursts of more than 500 particles

under 12 cm of lead are compared with the corresponding data obtained under 35 cm of iron in order to determine the dependence of burst frequency on atomic number; the results are in substantial agreement with production of these bursts by bremsstrahlung of the mesotron. Integral size-frequency distribution curves are also plotted for data obtained during a five-year period at Huancayo (3350-meters elevation) and at Cheltenham (72 meters) for bursts under 12 cm of lead. The Cheltenham data are compared with the theoretical calculations of Christy and Kusaka for burst production by mesotrons of spin 0, $\frac{1}{2}$, and 1 and it is concluded that either the spin 0 or the spin $\frac{1}{2}$ curve fits the experimental data but the evidence definitely excludes spin 1. The altitude dependence for burst under 12 cm of lead shows that the ratio of the burst frequencies at Huancayo and Cheltenham is constant for bursts up to 2400 particles, but increases sharply for still larger bursts. This increase is discussed on the basis that bursts under thick shields at higher altitudes may be caused either by extensive showers or by possible spin 1 mesotrons having so short a mean life that most of them fail to reach sea level.

INTRODUCTION

AS early as 1938 several investigators¹ pointed out that large cosmic-ray bursts which occur under thick shields are associated with the mesotron component of cosmic rays. Indeed, Christy and Kusaka² were able to demonstrate that the burst data of Schein and Gill³ were in substantial agreement with the theoretical calculations which they carried out for burst production for mesotrons of spin 0. For comparison with such theoretical calculations it is essential that burst data be obtained with an ionization chamber and shield of the proper geometry. A spherical ionization chamber surrounded by a uniform spherical shield of sufficient thickness to exclude all but the mesotron initiated bursts is an excellent geometrical arrangement. With a cylindrical chamber, however, comparison of experimental data with calculation is very difficult for the

number of particles observed in each burst will depend on the angle at which the particles intercept the chamber. Furthermore, if flat layers of shielding material are placed above the chamber, the effect of scattering of the burst particles in this absorber is also very difficult to calculate. For experiments concerned with burst production by mesotrons, a shield that uniformly surrounds the chamber on all sides is necessary since the mesotrons which can initiate large⁴ bursts are essentially isotropically distributed with respect to the zenith angle.

The importance of obtaining reliable burst data under thick⁵ shields lies in the fact that, at present, this is the most feasible method by which the electromagnetic interaction of high energy mesotrons with nuclei and electrons can be studied. In particular, such burst data constitute the only experimental evidence that the majority

¹ H. Euler, *Naturwiss.* **26**, 382 (1938); H. Euler and W. Heisenberg, *Ergeb. exakt. Naturwiss.* **17**, 1 (1938); M. Schein and P. S. Gill, *Phys. Rev.* **55**, 1111 (1939).

² R. F. Christy and S. Kusaka, *Phys. Rev.* **59**, 414 (1941).

³ M. Schein and P. S. Gill, *Rev. Mod. Phys.* **11**, 267 (1939).

⁴ In this paper only large cosmic-ray bursts are considered and these are arbitrarily taken as bursts containing more than 100 particles as measured in a spherical ionization chamber of 35-cm diameter.

⁵ By a thick shield, it is meant a shield of thickness sufficient to assure that the majority of the bursts observed under it are produced by mesotrons. This corresponds to a thickness of about 20 radiation units at sea level.

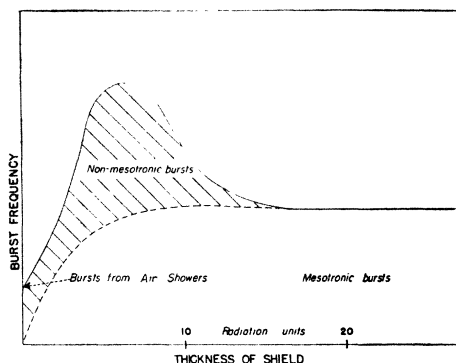


FIG. 1. Schematic curve representing a typical transition curve in which the relative burst frequency (in arbitrary units) is plotted against the thickness of the absorbing shield which surrounds the ionization chamber.

of the very large bursts under thick shields are initiated by the bremsstrahlung of a mesotron in the electromagnetic field of a nucleus. At energies above 10^{10} ev, this radiation process (bremsstrahlung) of the mesotron predominates over the close collision (knock-on process) of a mesotron with an electron. For both the bremsstrahlung and the knock-on process the forces which act are strongly spin-dependent, hence comparison of burst data with the theoretical results for burst production by mesotrons may yield an experimental determination of the spin of the mesotron. Such a comparison was first made by Christy and Kusaka² who compared the results of their calculations with the burst data³ obtained under a 12-cm lead shield at sea level. Because of the fact that bursts produced by the bremsstrahlung of the mesotron are actually photon initiated showers localized in the shield surrounding the ionization chamber, then in accordance with the cascade theory for such showers, the observed bursts should depend upon the square of the atomic number of the shielding material. In the present experiments, the dependence of the bursts upon atomic number was investigated by comparing the bursts under 35 cm of iron with the 12-cm lead burst data of Schein and Gill³ as well as with more recent data discussed in this paper.

Since practically all the large bursts observed at sea level under thick shields are due to mesotrons of energy greater than 10^{10} ev, there should be no altitude dependence for such bursts if bursts under thick shields at higher altitudes have the same origin as those at sea level. The

reason for this is that the mesotrons above 10^{10} ev having a lifetime of a 10^{-6} second undergo negligible decrease in intensity in traversing the atmosphere. However, it is well known³ that bursts under thick shields show a marked altitude dependence. For example, the number of bursts of more than 200 particles observed under 12 cm of lead at Huancayo, Peru (elevation 3350 meters) is 4.5 times greater than the number of bursts observed at sea level under the same experimental conditions. Thus one is led to the conclusion that there is present at higher altitudes a burst producing radiation which does not exist with measurable intensity at sea level. The fact that this radiation is so strongly absorbed in the atmosphere between Huancayo and sea level suggests that it may be associated with the high energy soft component of cosmic-rays. The theory of cascade showers initiated by primary electrons predicts that the extensive atmospheric showers⁶ should have a broad region which contains a high density of energetic electrons and photons. Recently, it was shown⁷ that at sea level such atmospheric showers actually possess a region (core) of sufficiently high particle density to record as a burst of more than 100 particles in an unshielded ionization chamber of 995-sq. cm cross-sectional area. More recently,⁸ it has been found that even when the ionization chamber was shielded with as much as 12 cm of lead, about 5 percent of the total bursts were observed to be coincident with a high density core of an atmospheric shower. This result is in agreement with the hypothesis that a few of the most energetic air showers may contain particles of energy sufficient to multiply under 12 cm of lead.

It is well known that if one varies from 0 to 20 radiation units the thickness of the shielding material around an ionization chamber at sea level, the burst frequency first increases from an initial finite value, then passes through a maximum, and finally attains a fairly constant value which is independent of any further increase in the thickness of the shield. Such a generalized

⁶ P. Auger, R. Maze, and T. Grivet-Meyer, *Comptes rendus* **206**, 1721 (1938); W. Kolhorster, J. Matthes, and E. Weber, *Naturwiss.* **26**, 576 (1938); P. Auger and R. Maze, *Comptes rendus* **207**, 228 (1938); P. Auger, R. Maze, P. Ehrenfest, Jr., and A. Freon, *J. de phys. et rad.* **10**, 39 (1939).

⁷ R. E. Lapp, *Phys. Rev.* **64**, 129 (1943).

⁸ R. E. Lapp, *Phys. Rev.* **64**, 254 (1943).

transition curve for large bursts is shown in Fig. 1. In order to facilitate the discussion of the origin of bursts under different thicknesses of shielding, three critical values of the thickness will be considered and the bursts corresponding to those measured under these thicknesses are designated as:

- (a) t_0 -bursts—those bursts observed in an unshielded chamber with negligible heavy material in the vicinity.
- (b) t_m -bursts—the bursts measured under a thickness of shield that gives the maximum burst frequency.
- (c) t_μ -bursts—those found under thick shields. (This thickness will have to be larger for higher altitudes in order to exclude those bursts originating from very energetic atmospheric showers.)

Three different explanations were offered to account for the origin of the t_0 -bursts. It was first⁹ suggested that these bursts could be produced by extremely large fluctuations in the cascade multiplication of an incident electron or photon. Second, Heisenberg¹⁰ proposed that these bursts might be created by a new type of multiple process, the so-called explosion shower. Finally, it was suggested that a large number of particles might be simultaneously incident upon an ionization chamber, giving rise to a burst in the chamber. Very recently,⁷ however, it was directly demonstrated that the t_0 -bursts were coincident with the high density core of an atmospheric shower as measured by the simultaneous coincidence of several G-M counter sets. This definitely proved that the last of the three suggestions is the correct one.

Thus, it is now established that the t_0 - and t_μ -bursts are of entirely different origin at sea level, the t_0 -bursts being produced by a core of an atmospheric shower and the t_μ -bursts being created by high energy single mesotrons. One would then think that the t_m -bursts would be of a complex nature, containing a mixture of t_0 - and t_μ -bursts with bursts of other (unknown) origin not being excluded.

⁹ D. K. Froman and J. C. Stearns, Rev. Mod. Phys. 10, 133 (1938).

¹⁰ W. Heisenberg, Zeits. f. Physik 113, 61 (1939).

APPARATUS

The ionization chamber used for the following experiments was a Carnegie model C meter which has been described elsewhere.¹¹ It will suffice to mention here that the chamber is a steel sphere of 17.5-cm inside radius with walls 1.25 cm thick. It is filled with very pure argon to a pressure of 50 atmospheres. As it is usually used, the chamber is mounted within a 3-mm walled spherical shell which is then filled with lead shot so that there is an equivalent of 12 cm of lead around the chamber. By means of a small auxiliary ionization chamber located within the main chamber, the ionization current due to cosmic radiation is compensated so that only the variations in the ionization due to cosmic rays are registered. A Lindemann electrometer was used to measure the ionization current and the image of the electrometer needle was focused upon a continuously moving strip of photographic paper. For the present experiments, the collecting electrode system of the chamber was automatically grounded every 15 minutes and once every hour a voltage of 0.40 volt was applied to the electrometer needle in order to check the sensitivity of the instrument. A synchronous clock drive fed the photographic paper through the recording camera at a rate of 8 cm/hr. and for convenience a time reference mark was registered on the paper every 6 hours.

A very simple system was devised to register coincidences of G-M counter sets on the same

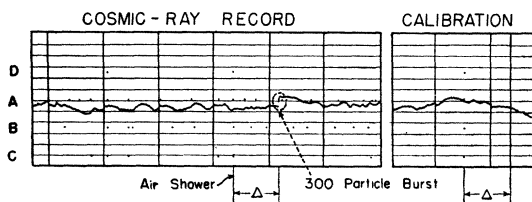


FIG. 2. A representative portion of the cosmic-ray ionization trace is shown. The distance between each of the vertical lines represents a time interval of 15 minutes. As explained in the text, each spot appearing on the record represents a coincidence of a G-M counter set, A, B, C, or D. These spots are off-set from the instantaneous ionization trace by an amount (Δ) which is determined by the calibration shown in the second frame from the right on the above record. In the fifth frame from the left a 300-particle burst is shown coincident with an extensive air shower.

¹¹ A. H. Compton, E. O. Wollan, and R. D. Bennett, Rev. Sci. Inst. 5, 415 (1934).

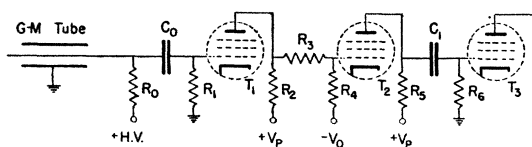


FIG. 3. The general principle of the twofold coincidence circuit is illustrated; only 1 arm of the circuit is shown since the other is identical and both arms are joined together by putting the last tubes in parallel in the usual manner. Circuit constants are: (resistances in megohms, condensers in micro-micro-farads)

$$R_0 = R_1 = 0.5 \quad R_2 = R_4 = R_5 = 0.1 \quad R_3 = 0.075 \quad R_6 = 0.010$$

Plate resistor of tube $T_3 = 0.2$ (not shown above)

$$C_0 = 100 \quad C_1 = 10$$

$$T_1, T_2, T_3 = 1LD5, 6SJ7, \text{ or } 7C7$$

Typical operating conditions: $V_p = 150$ volts, $V_{\text{Screen}} = 100$ volts, V_0 adjusted to give a grid potential on T_2 in the range of from -3 to -5 volts.

record as that on which the ionization trace was registered. Five pre-focused Mazda lamps were so mounted on the camera back that each lamp was focused onto a 0.007-inch aperture in a brass plate that rested against the back of the photographic paper in the camera. There was sufficient light intensity from this source so that when the lamps were flashed at rated voltage for $\frac{1}{10}$ of a second, a small spot was recorded on the photographic paper. Because of the design of the camera mechanism, it was not practical to locate the lamp apertures exactly at the point where the ionization trace was recorded; instead, the apertures were displaced $\frac{1}{2}$ inch from this point. To determine accurately this displacement Δ , the system was calibrated by simultaneously flashing all the lamps and interrupting the electrometer lamp circuit momentarily. This process is illustrated in Fig. 2 where an actual ionization record is shown. In the actual process of determining whether a burst were coincident with any of the G-M coincidences, it was found that the bursts and atmospheres showers were both so infrequent that it was relatively easy to detect the coincidences. It should be pointed out that the present arrangement for registering coincidences of G-M counter sets has distinct advantages for the investigation of atmospheric showers, for one can see at once for any given shower just how many and which G-M counter sets are triggered by the shower.

The twofold coincidence circuit used in these experiments has a resolving power of 1.2 microseconds and with the G-M counter tubes that

were used only one chance coincidence would occur every two hours. The circuit is given in Fig. 3 where it is seen that it is a three-stage amplifier with pure resistance coupling between the first and second stages. The low resolving time is attained by suitable choice of circuit constants between the second and third stage. The three-, four-, and fivefold circuits were of the usual design and in each circuit a sensitive relay in the plate circuit of the power output tube activated a micro-switch which in turn completed a lamp circuit in the camera back.

t_{μ} -BURSTS¹²

The t_{μ} -bursts were measured under a 35-cm iron shield,¹³ the details of which have already been given.⁸ The upper iron hemisphere was such that it presented a traversal distance of 35 cm for mesotrons which were radially incident upon the chamber. For most of the experiments, the apparatus was located on the top floor (greenhouse) of the Botany building on the campus of the University of Chicago. There was no heavy material above or to the side of the ionization chamber.

The data obtained during a time interval of 1754 hours are presented in Table I. Here the cumulative burst frequency ($\text{cm}^{-2} \text{sec.}^{-1}$) is given for different burst sizes¹⁴ (S). To obtain the burst frequency given in column 4 of Table I, the total number of bursts greater than a certain size (S) was divided by the product of the total elapsed

TABLE I. Integral number of bursts ($\text{cm}^{-2} \text{sec.}^{-1}$) with more than S particles produced in 35 cm of iron.

Burst size (in mm)	Burst size (S) (No. of particles)	Integral number of bursts (1754 hr.)	Burst frequency ($\text{cm}^{-2} \text{sec.}^{-1}$)
1.0- 2.0	100	372	$6.16 \cdot 10^{-8}$
2.0- 3.0	200	152	$2.52 \cdot 10^{-8}$
3.0- 4.0	300	78	$1.29 \cdot 10^{-8}$
4.0- 5.0	400	49	$8.12 \cdot 10^{-9}$
5.0- 6.0	500	42	$6.42 \cdot 10^{-9}$
6.0- 7.0	600	25	$4.14 \cdot 10^{-9}$
7.0- 8.0	700	18	$2.98 \cdot 10^{-9}$
8.0- 9.0	800	14	$2.32 \cdot 10^{-9}$
9.0-10.0	900	11	$1.82 \cdot 10^{-9}$
> 10	> 1000	5	$8.29 \cdot 10^{-10}$

¹² Both Dr. R. F. Christy and Dr. S. Kusaka were very generous in discussing the results of this experiment with the writer.

¹³ The author acknowledges the cooperation of Dr. W. P. Jesse in making the iron shield available for this experiment.

¹⁴ Unless otherwise specified, the burst size refers to the number of particles contained in the burst.

time (in seconds) multiplied by the cross-sectional area of the chamber (995 cm²). Schein and Gill⁸ have given the procedure for determining the number of particles in bursts for the type of ionization chamber used here. For the 35-cm iron experiment, the electrometer sensitivity was such that a 1-mm deflection corresponded to a burst of 100 particles. Before considering in detail the results given in Table I, it is necessary to proceed to a discussion of the relation of air showers to t_{μ} -bursts.

1. Relation to Air Showers

To detect any atmospheric showers which might be coincident with the t_{μ} -bursts, two sets of twofold coincidence arrangements of G-M counters were used. These G-M counters were placed on light wooden racks suspended over the ionization chamber. Each counter had an effective surface of 100 cm² and they were separated by distances of from 2 to 10 meters. As has already been reported,¹⁵ the coincidence experiments for the t_{μ} -bursts showed that they were not coincident with extensive air showers within the accuracy of the experiment. However, more recent experiments¹⁶ carried out with an equivalent thickness of 20 radiation units of lead around the ionization chamber showed that approximately 5 percent of the total bursts were coincident with air showers. There are two definite conclusions to be drawn from this result:

First, since the number of energetic air showers which could produce more than 100 particles below 20 radiation units is certainly small compared with the total number of the energetic air showers which are incident upon the chamber, one can conclude that most of these air showers at sea level do not contain particles of energy sufficient to traverse 20 radiation units of material. This is equivalent to stating that the cores of these air showers do not contain particles with energy greater than 2×10^{10} ev which is the minimum energy required for a single electron or photon to produce unit multiplication after traversing 20 radiation units.

Second, showers which do contain particles of energy more than 2×10^{10} ev capable of penetrating 20 radiation units of material are found to

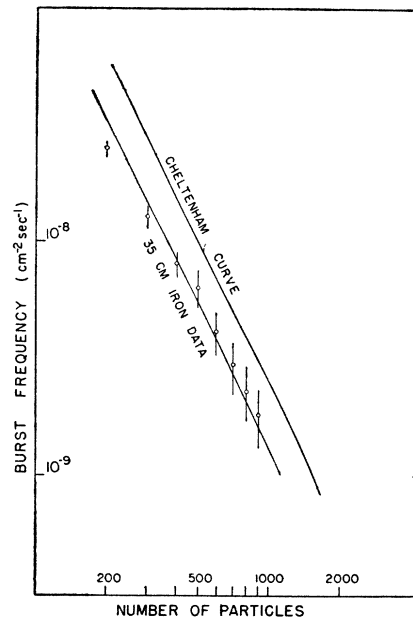


FIG. 4. The integral burst frequency (cm⁻² sec.⁻¹) for bursts observed at sea level under 35 cm of iron is plotted against the size of the bursts in number of particles. The Cheltenham curve represents a very accurate integral size-frequency distribution for t_{μ} -bursts observed under 12 cm of lead. Statistical errors are shown for the lower curve, those for the Cheltenham curve are shown in Fig. 6.

be extremely rare, occurring with a frequency of only one in four days as measured with the present experimental set-up. For such extremely rare showers, the primary particle initiating the shower, independent of its point of origin in the atmosphere, must have an extremely high energy which can be estimated from its high penetrating power and very low frequency of occurrence to be of the order of 10^{16} ev.¹⁷

The fact that only 5 percent of the bursts under thick shields are associated with air showers can be considered as direct evidence that the great majority of the t_{μ} -bursts at sea level are owing to single high energy particles. It was necessary to establish this point before proceeding to a comparison of the t_{μ} -burst data with the calculations of Christy and Kusaka for burst production by mesotrons. It also allows one to proceed with a discussion of the t_{μ} -burst data presented in Table I and facilitates the comparison of these data with other t_{μ} -burst data obtained by using a 12-cm lead shield around the ionization chamber.

¹⁵ R. E. Lapp, Phys. Rev. **63**, 60 (1943).

¹⁶ R. E. Lapp, Phys. Rev. **65**, 347 (1944).

¹⁷ L. Wolfenstein, Phys. Rev. **67**, 238 (1945).

2. Dependence on Atomic Number

In Fig. 4, the lower curve represents the data given in Table I for t_μ -bursts observed under 35 cm of iron. This curve, plotted on a double logarithmic scale, is called the cumulative or integral size-frequency distribution curve. It will be noted that the experimental points for the smallest burst sizes fall below the curve drawn in Fig. 4; this discrepancy has been noted by others and it is explained by the fact that many of the smallest bursts are confused with the statistical fluctuations of the cosmic-ray ionization occurring in the ionization chamber and are thus overlooked. That this explanation is actually correct is seen from the fact that the data of Steinke¹⁸ and Schmid¹⁹ for bursts of from 30 to 230 particles under thick shields are represented by a cumulative size-frequency distribution which is a direct continuation of the 35-cm iron curve in Fig. 4 and which has the same slope as this curve.

The cumulative size-frequency distribution curve for the t_μ -bursts under 35 cm of iron is represented by a simple power law of the form:

$$F(>S) = \text{const.}(1/S^\gamma), \quad (1)$$

where $F(>S)$ is the frequency of bursts of size greater than S ; S refers to the burst size in number of particles; γ has the value 2.0 ± 0.2 for $200 < S < 1000$.

In the same Fig. 4, there is also plotted the integral size-frequency distribution curve for bursts observed at Cheltenham²⁰ (72-meter elevation) with a Carnegie meter shielded by 12 cm of lead. This cumulative size-frequency distribution for bursts in lead can be compared with the 35-cm iron burst data to determine the dependence of burst frequency upon the atomic number of the shielding material. As pointed out in the *Introduction*, the t_μ -bursts originate in the shielding material surrounding the ionization chamber as a result of the interaction of mesotrons with this material. Two different mechanisms are involved in this interaction whereby a mesotron

transfers a large fraction of its energy to an electron or photon. First, a high energy mesotron may make a very close collision with an electron (knock-on process) and thus transfer to the electron a large part of its energy. Second, a photon may be produced by the electromagnetic interaction of a mesotron with a nucleus and thus carry away most of the mesotron's energy (bremsstrahlung process). The cross sections for these processes were calculated by Christy and Kusaka²¹ and others.²²

Comparison of the 35-cm iron distribution curve with the 12-cm lead curve can be made on the following basis. The cascade theory predicts that if the initial energy of the photon (for t_μ -bursts produced by bremsstrahlung) initiating the burst in lead or iron is measured in units of the critical shower energy (β) of the shielding material, and if the thickness of the shield is measured in radiation units, then the burst frequency should be nearly independent of the nature of the shielding material for thicknesses greater than 20 radiation units. As a result, for bursts of more than 500 particles ($E > 5 \times 10^{10}$ ev) one should, therefore, expect that the size-frequency distribution curves for bursts measured under an equivalent thickness of lead and iron would be parallel to each other but horizontally displaced by an amount equal to the ratio of the critical energies: $\beta_{Fe}/\beta_{Pb} = 22.4/8 = 2.8$. Actually one finds that the curves in Fig. 4 are essentially parallel but are displaced from one another by a factor of only 1.4 for bursts greater than 500 particles which are practically all initiated by the bremsstrahlung process as will be shown later. That the experimentally determined ratio is considerably smaller than the predicted ratio is caused by the fact that the t_μ -burst data for lead are obtained by using an ionization chamber with a 1.25-cm iron wall surrounded by 10.7 cm of lead whereas the t_μ -burst data for iron is obtained with a homogeneous iron shield. Thus for the lead (Cheltenham) burst data a transition effect occurs which results in an appreciable absorption of the burst particles which are produced in the

¹⁸ E. G. Steinke and H. Schmid, *Zeits. f. Physik* **115**, 740 (1940).

¹⁹ H. Schmid, *Zeits. f. Physik* **117**, 452 (1941).

²⁰ Dr. Jno. A. Fleming of the Carnegie Institution at Washington, D. C. kindly made available to the author some five years of burst data from the Cheltenham, Maryland cosmic-ray station. In Fig. 4 only the smoothed curve for these data is shown; the statistical errors for the experimental points are given in Fig. 6.

²¹ R. F. Christy and S. Kusaka, *Phys. Rev.* **59**, 405 (1941).

²² H. J. Bhabha, *Proc. Roy. Soc.* **164**, 257 (1938); H. S. W. Massey and H. C. Corben, *Camb. Phil. Soc.* **35**, 463 (1939); J. R. Oppenheimer, H. Snyder, and R. Serber, *Phys. Rev.* **57**, 75 (1940).

TABLE II. Integral number of bursts (cm⁻² sec.⁻¹) with more than *S* particles produced in 20 radiation units of material calculated for mesotrons of spin 0, ½, and 1. The burst frequencies due to knock-ons and bremsstrahlung in lead are given in (a) and (b) while those for iron are given in (c) and (d). The total frequencies in lead are found in (e) and (f), respectively.

Lead				Lead			
β <i>S</i> ×10 ⁹	(a) Knock-on Bursts (cm ⁻² sec. ⁻¹)			(b) Bremsstrahlung Bursts (cm ⁻² sec. ⁻¹)			
	Spin 0	Spin ½	Spin 1	Spin 0	Spin ½	Spin 1	
1	6.8 · 10 ⁻⁸	8.7 · 10 ⁻⁸	1.2 · 10 ⁻⁷	2.0 · 10 ⁻⁷	3.2 · 10 ⁻⁷	1.0 · 10 ⁻⁶	
2	1.3 · 10 ⁻⁸	1.8 · 10 ⁻⁸	3.2 · 10 ⁻⁸	7.3 · 10 ⁻⁸	1.2 · 10 ⁻⁷	4.8 · 10 ⁻⁷	
4	2.3 · 10 ⁻⁹	3.3 · 10 ⁻⁹	8.1 · 10 ⁻⁹	2.2 · 10 ⁻⁸	3.8 · 10 ⁻⁸	2.1 · 10 ⁻⁷	
8	3.5 · 10 ⁻¹⁰	5.4 · 10 ⁻¹⁰	2.1 · 10 ⁻⁹	6.0 · 10 ⁻⁹	1.0 · 10 ⁻⁸	8.7 · 10 ⁻⁸	
16	5.1 · 10 ⁻¹¹	8.1 · 10 ⁻¹¹	5.5 · 10 ⁻¹⁰	1.4 · 10 ⁻⁹	2.5 · 10 ⁻⁹	3.3 · 10 ⁻⁸	
32	7.1 · 10 ⁻¹²	1.2 · 10 ⁻¹¹	1.5 · 10 ⁻¹⁰	2.9 · 10 ⁻¹⁰	5.1 · 10 ⁻¹⁰	1.2 · 10 ⁻⁸	
64	9.7 · 10 ⁻¹³	1.6 · 10 ⁻¹²	3.9 · 10 ⁻¹¹	5.0 · 10 ⁻¹¹	9.0 · 10 ⁻¹¹	3.7 · 10 ⁻⁹	

Iron				Iron			
β <i>S</i> ×10 ⁹	(c) Knock-on Bursts (cm ⁻² sec. ⁻¹)			(d) Bremsstrahlung Bursts (cm ⁻² sec. ⁻¹)			
	Spin 0	Spin ½	Spin 1	Spin 0	Spin ½	Spin 1	
1	2.1 · 10 ⁻⁷	2.7 · 10 ⁻⁷	3.8 · 10 ⁻⁷	2.0 · 10 ⁻⁷	3.2 · 10 ⁻⁷	1.0 · 10 ⁻⁶	
2	4.1 · 10 ⁻⁸	5.6 · 10 ⁻⁸	1.0 · 10 ⁻⁷	7.3 · 10 ⁻⁸	1.2 · 10 ⁻⁷	4.8 · 10 ⁻⁷	
4	7.2 · 10 ⁻⁹	1.0 · 10 ⁻⁸	2.5 · 10 ⁻⁸	2.2 · 10 ⁻⁸	3.8 · 10 ⁻⁸	2.1 · 10 ⁻⁷	
8	1.1 · 10 ⁻⁹	1.7 · 10 ⁻⁹	6.6 · 10 ⁻⁹	6.0 · 10 ⁻⁹	1.0 · 10 ⁻⁸	8.7 · 10 ⁻⁸	
16	1.6 · 10 ⁻¹⁰	2.5 · 10 ⁻¹⁰	1.8 · 10 ⁻¹⁰	1.4 · 10 ⁻⁹	2.5 · 10 ⁻⁹	3.3 · 10 ⁻⁸	
32	2.2 · 10 ⁻¹¹	3.8 · 10 ⁻¹¹	4.7 · 10 ⁻¹⁰	2.9 · 10 ⁻¹⁰	5.1 · 10 ⁻¹⁰	1.2 · 10 ⁻⁸	
64	3.0 · 10 ⁻¹²	5.0 · 10 ⁻¹²	1.2 · 10 ⁻¹⁰	5.0 · 10 ⁻¹¹	9.0 · 10 ⁻¹¹	3.7 · 10 ⁻⁹	

Lead				Iron			
β <i>S</i> ×10 ⁹	(e) Knock-on + Bremsstrahlung Bursts (cm ⁻² sec. ⁻¹)			(f) Knock-on + Bremsstrahlung Bursts (cm ⁻² sec. ⁻¹)			
	Spin 0	Spin ½	Spin 1	Spin 0	Spin ½	Spin 1	
1	2.7 · 10 ⁻⁷	4.1 · 10 ⁻⁷	1.1 · 10 ⁻⁶	4.2 · 10 ⁻⁷	5.9 · 10 ⁻⁷	1.4 · 10 ⁻⁶	
2	9.0 · 10 ⁻⁸	1.4 · 10 ⁻⁷	5.1 · 10 ⁻⁷	1.1 · 10 ⁻⁸	1.8 · 10 ⁻⁷	5.8 · 10 ⁻⁷	
4	2.5 · 10 ⁻⁸	4.1 · 10 ⁻⁸	2.2 · 10 ⁻⁷	2.9 · 10 ⁻⁸	4.8 · 10 ⁻⁸	2.3 · 10 ⁻⁷	
8	6.4 · 10 ⁻⁹	1.1 · 10 ⁻⁹	8.9 · 10 ⁻⁸	7.1 · 10 ⁻⁹	1.2 · 10 ⁻⁸	9.3 · 10 ⁻⁸	
16	1.5 · 10 ⁻⁹	2.6 · 10 ⁻⁹	3.3 · 10 ⁻⁸	1.6 · 10 ⁻⁹	2.8 · 10 ⁻⁹	3.5 · 10 ⁻⁸	
32	2.9 · 10 ⁻¹⁰	5.2 · 10 ⁻¹⁰	1.2 · 10 ⁻⁸	3.1 · 10 ⁻¹⁰	5.5 · 10 ⁻¹⁰	1.2 · 10 ⁻⁸	
64	5.0 · 10 ⁻¹¹	9.2 · 10 ⁻¹¹	3.7 · 10 ⁻⁹	5.3 · 10 ⁻¹¹	9.5 · 10 ⁻¹¹	3.7 · 10 ⁻⁹	

lead shield. Christy and Kusaka made a correction for this effect by calculating an effective absorbing thickness of iron. This correction was applied by introducing a critical energy β = 13 × 10⁶ ev instead of β = 8 × 10⁶ ev which is the value for pure lead. Using this value for the critical energy for the lead curve in Fig. 4, one arrives at the following ratio :

$$\frac{\beta_{Fe}}{\beta_{Pb-Fe}} = \frac{22.4 \times 10^6 \text{ ev}}{13 \times 10^6 \text{ ev}} = 1.7,$$

which is in as good agreement with the experimental value of 1.4 as can be expected if one considers the fact that statistically exact data for bursts greater than 500 particles require at least several years for collection. On the other hand, changing the critical energy from an estimated value of 13 × 10⁶ ev to 16 × 10⁶ ev results in very good agreement between the theoretical and ex-

perimental values for the burst frequencies in iron and in lead. Since the dependence of burst frequency upon atomic number is thus in first approximation in agreement with the predictions of the cascade theory, this definitely indicates that t_μ-bursts greater than 500 particles must be predominantly produced by the bremsstrahlung process.

3. The Spin of the Mesotron

As a result of the experimental data presented above, one is now in a position to compare the t_μ-burst data with the theoretical calculations for burst production by knock-on and bremsstrahlung processes. The recent and more extensive burst data from Cheltenham permit this comparison to be made even for very large bursts (S > 1000 particles). Table II contains the calculated values for burst frequency as a function of the quantity β*S* where β represents the critical energy of the shielding element and *S* is the burst size; the values for lead are taken directly from Christy and Kusaka² while the values for iron were calculated by the author. Sections (e) and (f) in Table II give the total frequency for bursts in lead and in iron for mesotrons of spin 0, ½, and 1. The burst frequencies are given for corresponding values of the quantity β*S* for the following reason : if one plots the calculated burst frequency *versus* the quantity β*S*, it follows from the cascade theory of showers that experimental data for any value of β can be directly compared with this theoretical curve. This comparison will be valid for all values of β*S* > 5 × 10⁹ where the effect of knock-on processes is negligible (see Table II). From the data given in Table II, the percentage of bursts in iron and in lead due to knock-ons (from mesotrons of spin 0 and ½) is calculated as a function of β*S* and the results are given in Fig. 5. Since, however, the Cheltenham which are to be compared with the theoretical burst frequencies in Table II involve a transition effect which is introduced by the 1.25-cm iron chamber wall, one has to consider a curve which is intermediate between the lead and the iron curves (Fig. 5) in order to see the contribution of bursts due to knock-ons. Taking into consideration this transition effect, the lead-iron curve (Fig. 5) shows that for β*S* = 1.5 × 10⁹ corresponding to a 200-particle burst the percentage of

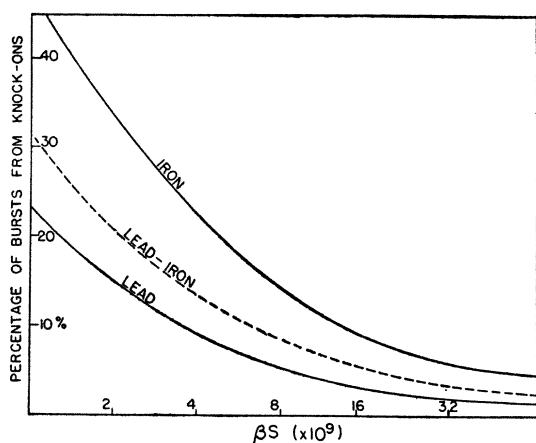


FIG. 5. The contribution to the total t_{μ} -burst frequency by bursts produced by knock-ons from mesotrons of spin 0 and $\frac{1}{2}$ is illustrated. The quantity βS is the product of the critical shower energy β multiplied by the size S as given by the number of particles in the burst. The dotted curve labeled Lead-Iron is drawn for burst data obtained with 1.25 cm of iron and 11 cm of lead.

bursts due to knock-ons is 25 percent while for a 600 particle burst it is only 10 percent. Thus for bursts larger than about 500 particles the effect of knock-ons does not seriously affect the comparison of the theoretical burst frequencies with the experimental data as was discussed earlier in connection with the dependence of burst frequency on atomic number.

A direct comparison of the theoretical values for burst production by mesotrons given in Table II is now made with the experimental t_{μ} -burst data for the Cheltenham station. This comparison is given in Fig. 6, where the solid curves represent the theoretical curves calculated for t_{μ} -bursts produced by mesotrons of spin 0, $\frac{1}{2}$, and 1. On the same graph, the total knock-on contribution to the burst frequency averaged for spin 0 and $\frac{1}{2}$ is plotted (see the lower dotted curve). The Cheltenham data have been plotted in Fig. 6 with the estimated value of $\beta = 13 \times 10^6$ ev. It is seen that these experimental points are in excellent agreement with the size-frequency distribution curve for bursts produced by mesotrons of spin 0. However, in discussing the dependence of burst frequency on atomic number it was noted that a value of $\beta = 16 \times 10^6$ ev yielded better agreement between theory and experiment. The effect of using this higher value of β for the Cheltenham data would be to shift the experimental points upward on the graph to a position

intermediate between the spin 0 and spin $\frac{1}{2}$ curves. On the other hand, it has to be noted that in the theoretical calculation of the spin $\frac{1}{2}$ curve, a mesotron mass $= 200m_e$ (m_e = electron mass) was used; by assuming a larger mesotron mass, the spin $\frac{1}{2}$ curve can be shifted downward to coincide with the experimental points for the Cheltenham data. For a value of $\beta = 13 \times 10^6$ ev, such a displacement of the spin $\frac{1}{2}$ curve would require a mesotron mass $= 230m_e$. At present, the mass of the mesotron is not even determined to be within these limits (177 to $230m_e$) and, indeed, it has not been experimentally demonstrated that the mesotron is a particle of unique mass.

Therefore, on the basis of the present experimental results, it does not seem possible to determine whether the t_{μ} -bursts observed at sea level are produced by mesotrons of spin 0 or if they originate from spin $\frac{1}{2}$ mesotrons. The very great divergence of the experimental data from the theoretical values for burst production by mesotrons of spin 1 does show, however, that at sea level no appreciable fraction of the t_{μ} -bursts can be due to mesotrons of spin 1.²³

4. Comparison with Underground Data

If, in place of the βS scale used for the abscissa in Fig. 6, one is to substitute an energy scale, then one has to calculate the average energy per burst particle. This calculation is complicated by the fact that whenever a burst is measured in the chamber, only a single measurement is made of the total number of ions collected in the burst. From this measurement the number of particles in the burst has to be derived. It has been estimated² that for the chamber used here, the most probable energy per burst particle is 6β . If this value of 6β is used and β is taken to be 13×10^6 ev, then the probable energy per burst particle is 7.8×10^7 ev. This enables one to assign a definite energy scale to the abscissa of Fig. 6. On the assumption²⁴ that the fractional energy transfer of a high energy mesotron to an electron or photon is independent of its energy, the size-frequency distribution for t_{μ} -bursts should represent the integral energy spectrum for mesotrons at sea level.

The underground cosmic-ray intensity meas-

²³ R. E. Lapp, Phys. Rev. **64**, 255 (1943).

²⁴ J. R. Oppenheimer, Rev. Mod. Phys. **11**, 264 (1939).

urements²⁵ also provide an approximate evaluation of the integral energy spectrum for mesotrons at sea level and it is of interest to compare Wilson's depth curve with the Cheltenham curve. Assuming that the particles which Wilson measured were mesotrons which lose energy predominantly by ionization loss, one can assign an energy scale to the depth curve. It is understood that for exact calculation of the energy, losses other than ionization must be considered.²⁶ The Cheltenham curve and Wilson's depth curve are plotted in Fig. 7. For these curves, the same energy scale is used but the ordinates are chosen so as to bring the curves arbitrarily close together to facilitate comparison of their slopes. For energies greater than 6×10^{10} ev corresponding to 250 meters of water equivalent, the slopes of the two curves are nearly the same, indicating that the cosmic radiation producing the large t_μ -bursts at sea level consists of the same particles (mesotrons) which are able to penetrate deep into the earth's surface.

5. Altitude Dependence

To investigate the origin of the t_μ -bursts occurring at higher altitudes, burst data collected over five years at Huancayo (altitude 3350 meters) were studied. A preliminary analysis²⁷ of these data has been completed, and the integral size-frequency distribution curve derived from these data is given in Fig. 8 where the Cheltenham curve is given again for purposes of comparison. Comparison of the curves given in Fig. 8 is best accomplished by taking the ratio of the frequencies at the two given altitudes and plotting this ratio as a function of burst size. This is done in Fig. 9. It will be noticed that this ratio is essentially constant for burst smaller than 2400 particles and thereafter it increases almost linearly. Schein and Gill³ have discussed this phenomenon at some length and if one compares their curve for the ratio of burst frequencies at the same two altitudes with Fig. 9, it is noted that the point at which the ratio departs from being constant is shifted to larger burst sizes for the curve given in Fig. 9. This is caused by the

fact that more data have been incorporated into the curve in Fig. 9 and greater statistical accuracy for the largest burst sizes is thus attained.

In order to discuss in detail the increase in the ratio of burst frequencies at the two given altitudes, the theoretical curves for burst production by mesotrons of different spin are again considered. For this purpose, the Huancayo data were given on the same graph in Fig. 6. From these curves, it is apparent that if spin 1 mesotrons exist at higher altitudes and become decreasingly important at lower altitudes (since spin 1 mesotrons are assumed to be short lived and therefore are rapidly absorbed in the atmosphere between the two altitudes), then the ratio of the burst frequencies at the two altitudes should increase with energy as given by the

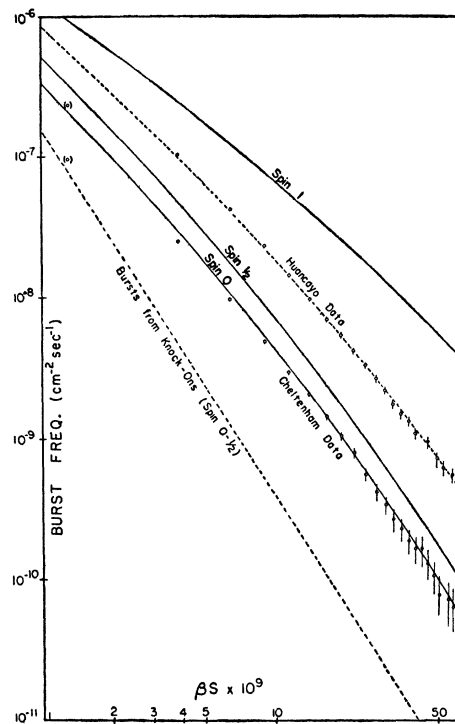


FIG. 6. The integral size-frequency distributions (solid curves above) for burst production by mesotrons of spin 0, $\frac{1}{2}$, and 1 as given in Table II are plotted as a function of the quantity βS . β is the critical shower energy and S is the burst size in number of particles. With this abscissa, the point $\beta S = 5 \times 10^9$ corresponds to a burst of 400 particles where β is taken as 13×10^6 ev. In addition, the burst frequency due to knock-ons for spin 0 or $\frac{1}{2}$ is given by the lower dotted curve. Two sets of experimental data are plotted for comparison with the theoretical curves; the lower set (Cheltenham Data) gives the burst frequency for sea level, while the upper set (Huancayo Data) represents the frequency for an altitude of 3350 meters.

²⁵ V. C. Wilson, Phys. Rev. **53**, 337 (1938); J. Clay and A. V. Gemert, Physica **6**, 497 (1939); A. Ehmert, Zeits. f. Physik **106**, 751 (1937).

²⁶ D. Lyons, Physik. Zeits. **42**, 166 (1941).

²⁷ M. Schein and R. E. Lapp, Phys. Rev. **65**, 63 (1944).

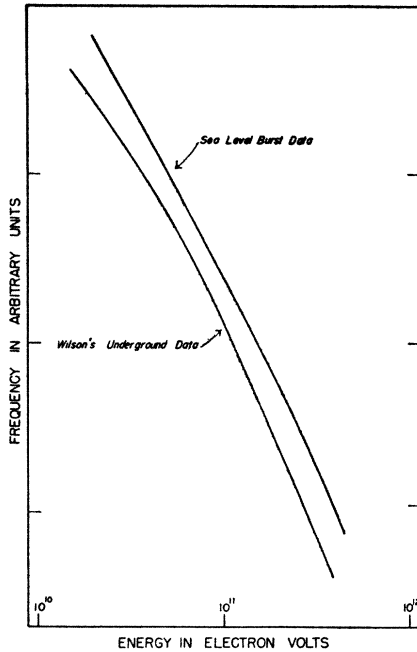


FIG. 7. The integral size-frequency distribution curve for Cheltenham (upper curve labeled Sea Level Burst Data) is compared with the underground data of V. C. Wilson (see reference 25). For the purpose of comparison the abscissa is given in terms of energy measured in electron volts. The two curves are plotted arbitrarily close together to facilitate comparison of their slopes.

number of particles in the bursts. From nuclear theory, it is predicted²⁸ that spin 1 mesotrons should have a lifetime of about 10^{-9} second.

Another explanation was suggested³ to account for this phenomenon by considering the possibility that energetic air showers might give rise to t_μ -bursts at higher altitudes. Since the number of these air showers was found to be extremely small at sea level and since air showers of very high energy (10^{16} ev) should increase considerably slower¹⁷ with altitude than the corresponding burst frequencies, it seems rather improbable that burst production by such giant air showers could account for the observed altitude dependence.

t_0 -BURSTS

Several observers^{18,29} have noted that the frequency of large bursts measured in thin-walled

²⁸ W. Heisenberg, *Kosmische Strahlung* (Verlagsbuchhandlung, Julius Springer, Berlin, 1943).

²⁹ D. Heyworth and R. D. Bennett, *Phys. Rev.* **50**, 589 (1936); H. Nie, *Zeits. f. Physik* **99**, 453 (1936); C. G. Montgomery and D. D. Montgomery, *Phys. Rev.* **56**, 640 (1939).

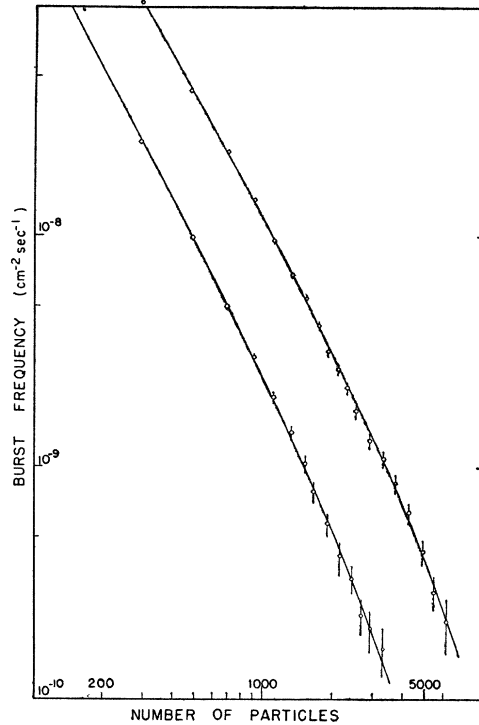


FIG. 8. Comparison of the integral size-frequency burst distributions for Cheltenham (72-m elevation) and Huancaayo (3350-m elevation). Both size-frequency distributions incorporate about 5 years of burst data; the upper curve for Huancaayo is based on data from 35,000 bursts larger than 200 particles.

ionization chambers depends rather strongly on the amount of dense material which is close to the chamber. For results that can be clearly interpreted it is essential that experiments on bursts in thin-walled chambers, *viz.*, t_0 -bursts, be carried out in a location where the horizon is not obstructed by dense material. One should use a structure which has not only a thin roof but also has thin walls. The experiments on t_0 -bursts described here were carried out in the glass greenhouse located on the fifth floor of the Botany building on the campus of the University of Chicago. The greenhouse roof and side structure were entirely of glass construction with light metal reinforcement and there were no nearby buildings to obstruct the horizon. Racks used to support the G-M counters used in these experiments were of light wooden construction.

1. Relation to Air Showers

The primary object of the t_0 -bursts experiment was to determine whether or not these bursts

were coincident with air showers. Some of the results of these coincidence experiments have already been published.⁷ As the initial set-up for the coincidence experiments, two twofold coincidence sets of G-M counter tubes were used to detect air showers. These were used in order to have the highest probability for detecting extensive air showers. It was then found that the majority of the t_0 -bursts were coincident with a simultaneous triggering of both twofold sets, but there was a small number of t_0 -bursts that were accompanied by a triggering of only 1 set and a few which were not coincident with a triggering of either set. The quantitative investigation of these t_0 -bursts is made difficult because of their low frequency, only 1 or 2 such bursts being recorded per day. For the purpose of investigating more accurately the relation of the t_0 -bursts to air showers, three additional counter sets were utilized. Using these additional counter sets (a threefold, a fourfold, and a fivefold coincidence set) large t_0 -bursts were observed which were coincident with a simultaneous triggering of all 5 of the G-M sets.³⁰ The data obtained from these coincidence experiments may be summarized as follows:

- (1) The larger the burst size, the greater is the probability that the burst is coincident with an extensive shower.
- (2) In most cases, the larger bursts trigger more of the G-M sets than the smaller bursts.
- (3) About 1/7 of the total bursts³¹ were not coincident with a triggering of any of the G-M sets.

These results are discussed later in this section in connection with the density distribution of particles in atmospheric showers. It may be pointed out at this time, however, that those t_0 -bursts which were not coincident with extensive showers might be produced by narrow angle air showers or by local showers generated in the small amount of dense material in the vicinity of chamber.

2. Size-Frequency Distribution

Table III shows the t_0 -burst data obtained during a time interval of 2063 hours. Since the

³⁰ The G-M sets were arranged as shown in Fig. 1 of reference 7.

³¹ It is not possible to express this fraction more exactly because in a completely unshielded condition, the ionization chamber records considerable fluctuation in the cosmic-ray ionization and due to this fact, many of the smaller bursts may be overlooked.

size-frequency distribution curve for these data has already been given,⁷ it is not reproduced separately³² here. It is obvious that the 1.25-cm iron wall of the chamber will tend to produce some multiplication of the particles which are incident on it. This wall is equal to 0.7 radiation units (r.u.) and this thickness of material is sufficient also to cause some of the incident particles to be absorbed. If the incident particles are selectively more absorbed than they are multiplied by the 0.7 r.u. there will be correspondingly fewer small bursts recorded, thus causing a flattening of the integral size-frequency distribution curve. In comparing the t_0 -burst data obtained with different ionization chambers, it must be born in mind that the following factors will have an appreciable effect on the observed burst frequency:

- (1) The thickness and material of the chamber wall.
- (2) The altitude at which the t_0 -bursts are measured.
- (3) The geometry of the ionization chamber.
- (4) Presence of dense material in the vicinity of the chamber.

In general, it is almost impossible to accurately correct t_0 -burst data for variations in these four factors and it is therefore very difficult to compare the burst data of different experimenters. Migdal³³ and others³⁴ have directly compared various t_0 -burst data. An extensive survey of the litera-

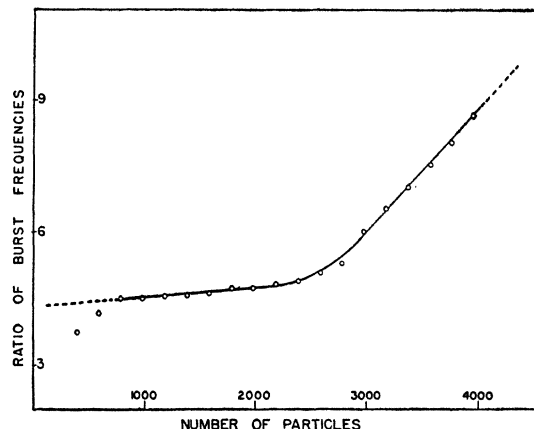


FIG. 9. Ratio of the burst frequencies at Huancayo and Cheltenham as a function of burst size.

³² The t_0 -burst curve is shown later in Fig. 12 of this paper.

³³ A. Migdal, J. Phys. U.S.S.R. 9, 183 (1945).

³⁴ G. Hoffmann, Zeits. f. Physik 119, 35 (1942); K. L. Kingshill and L. G. Lewis, Phys. Rev. 68, (1946).

TABLE III. Integral number of bursts ($\text{cm}^{-2} \text{sec.}^{-1}$) with more than S particles produced in 1.25 cm of iron.

Burst size (in mm)	Burst size (S) (No. of particles)	Integral number of bursts (2063 hr.)	Burst frequency ($\text{cm}^{-2} \text{sec.}^{-1}$)
1.0-1.5	100	170	$2.30 \cdot 10^{-8}$
1.5-2.5	150	138	$1.86 \cdot 10^{-8}$
2.5-3.5	250	84	$1.14 \cdot 10^{-8}$
3.5-4.5	350	43	$5.82 \cdot 10^{-9}$
4.5-5.5	450	24	$3.25 \cdot 10^{-9}$
5.5-6.5	550	13	$1.76 \cdot 10^{-9}$
6.5-7.5	650	10	$1.35 \cdot 10^{-9}$
7.5-8.5	750	8	$1.08 \cdot 10^{-9}$
8.5-9.5	850	6	$8.12 \cdot 10^{-10}$
>9.5	>950	5	$6.75 \cdot 10^{-10}$

ture has revealed a lack of t_0 -burst data with which the data obtained here could be compared for burst sizes greater than 200 particles. Using a chamber with 0.3-mm steel walls but otherwise similar to the one used here, Kingshill and Lewis³⁴ have recently obtained t_0 -burst data for bursts smaller than 200 particles. It is interesting to note that for 200 particle bursts, they found a frequency of 1.1×10^{-8} burst $\text{cm}^{-2} \text{sec.}^{-1}$ as compared with the value 1.6×10^{-8} burst $\text{cm}^{-2} \text{sec.}^{-1}$ found here for bursts of the same size. This approximate agreement indicates that the 1.25-cm iron wall in the Carnegie chamber does not drastically affect the observed burst frequency apparently because there is a compensation between the number of particles being absorbed in the iron and those being multiplied by it.

3. Density vs. Extension in Air Showers

Extensive air showers have been generally investigated by determining the coincidence counting rate for two or more G-M counters as a function of the lateral distance separating the counters. From these and similar experiments in which the extension of the shower was the experimental quantity observed, values were deduced both for the density of particles in the shower as well as for the energy of these particles. These values, however, could only be obtained by using the cascade theory applied to multiplicative processes for electrons and photons, for which an energy spectrum was assumed to be valid to energies up to 10^{16} ev. It is now known that these first³⁵ calculations on cascade multiplication in the atmosphere neglected important considera-

³⁵ H. Euler, *Zeits. f. Physik* **116**, 73 (1940).

tions. Such factors, as the zenith angle dependence and the diffusion effect³⁶ for electrons and photons in the shower cannot be neglected, and if they are taken into consideration, the results then obtained¹⁷ are in disagreement with the assumption that most of these showers could originate close to the top of the earth's atmosphere.

The coincidence experiments on t_0 -bursts described here show definitely that the great majority of the large bursts observed in unshielded ionization chambers at sea level are produced by a high density core of an atmospheric shower striking the chamber. For the range of burst sizes observed, the density of particles in the cores of these showers is of the order of 10^3 to 10^4 particles per square meter. If the region of such high particle density in an atmospheric shower had considerable extension, then it would have been observed that all of the G-M sets would have been simultaneously triggered when such a shower was centered upon the ionization chamber. The coincidence data show that many of the t_0 -bursts did not trigger all of the G-M sets, thus indicating that high density cores of such showers do not exhibit very great lateral extension. This point will be amplified after considering the t_m -burst coincidence data.

t_m -BURSTS

For large cosmic-ray bursts, it is well known that a maximum burst frequency is obtained for a thickness of shielding material around the chamber equivalent to 6 or 7 radiation units. For iron, 7 r.u. corresponds to about 12 cm.³⁷ The 12-cm iron shield was made up of two mating hemispherical caps of 3-cm wall thickness which fitted around the chamber and in addition a uniform layer of No. 22 iron shot equivalent to 7.7 cm of solid iron was placed around these caps.

1. Relation to Air Showers

For the t_m -burst coincidence experiments, the G-M counter sets were arranged as shown in Fig. 10. By use of this arrangement of counters, coincidence data were collected for 568 hours during which time 197 bursts were observed. In

³⁶ J. A. Richards and L. W. Nordheim, *Phys. Rev.* **61**, 735 (1942).

³⁷ H. Nie (reference 29) reports that he finds a maximum frequency of bursts in iron for a thickness between 10 and 15 cm.

Table IV, these data are presented and it is seen that of the total of 197 t_m -bursts, 39 were observed to be coincident with one or more of the G-M counter coincidences. Additional information on these coincident bursts is given in Table V in which the number of coincident bursts is tabulated as a function of the burst size. Moreover, the total number of t_m -bursts for each burst size is also listed in the Table V and the ratio of coincident bursts to total bursts is given as a function of the burst size.

Analysis of the data presented in Tables IV and V allows the following conclusions to be drawn. Coincident t_m -bursts have the highest probability for triggering the threefold G-M set C, the next highest probability for fourfold set D, and the least for twofold set B. Thus while the twofold set should have the highest probability for detecting an extensive shower, it has a lower rate of coincidence with the t_m -bursts than do the three and fourfold G-M sets which essentially measure a higher density but less extensive shower. This means that a large fraction of the t_m -bursts have their origin in the incidence of narrow air showers on the ionization chamber. In good agreement with conclusion are the data of Kingshill and Lewis³⁴ who observed very infre-

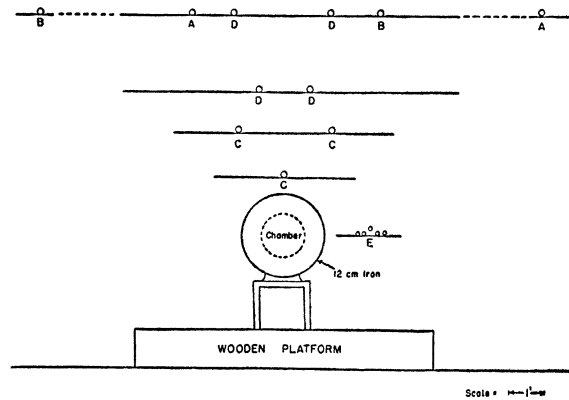


FIG. 10. Arrangement of ionization chamber and G-M counters for the t_m -burst experiment. G-M tube dimensions are: G-M A 2''×19'', B 2''×15'', C 2''×10'', D 2''×10'', E 1''×10''.

TABLE IV. G-M counter coincidence data for t_m -bursts.

Counter set—Type	No. of coincident t_m -bursts >150 particles
B twofold	18
C threefold	34
D fourfold	30
E fivefold	10
Total —	39

Ratio: $\frac{\text{total coincident bursts}}{\text{total bursts}} = \frac{39}{197} = 20 \text{ percent}$

TABLE V. G-M counter coincidence data for t_m -bursts as a function of burst size.

Burst size	Total bursts	Coincident bursts	Ratio
2	58	13	0.22
3	48	5	0.10
4	41	6	0.15
5	19	3	0.16
6	7	1	0.14
7	4	2	0.50
8	9	4	0.45
9	2	1	0.50
10	2	1	0.50
>10	7	3	0.43

quent coincidences between t_0 -bursts in two thin-walled chambers separated by a distance of one meter. Furthermore, it is evident from Table V that the probability for a t_m -burst to be coincident with an air shower increases with increasing burst size. For a burst larger than 500 particles, there is about a 50 percent probability for the burst to be coincident with an air shower. This can be interpreted as meaning that these air showers not only have higher densities of particles in their cores and thus trigger the G-M counter sets, but also contain particles of higher energy necessary to traverse the 12 cm of iron and produce large bursts in the chamber.

So far, the origin of only 20 percent of the t_m -bursts has been discussed. Before proceeding to a discussion of the other t_m -bursts, it is necessary to consider the integral size-frequency distribution curve for the t_m -bursts in relation to the t_0 - and t_μ -bursts so that the transition effect for large bursts in iron may be studied.

2. Size-Frequency Distribution

Burst data collected during 1411 hours of recording time are tabulated in Table VI. For these observations, the Lindemann electrometer was operated at a higher sensitivity than for the t_0 - and t_μ -experiments so that more data for the smaller bursts were obtained as indicated by the fact that during the 1411 hours, 965 bursts were recorded. The integral size-frequency distribution curve for these data is plotted in Fig. 11. This t_m -burst curve conforms to an inverse exponential

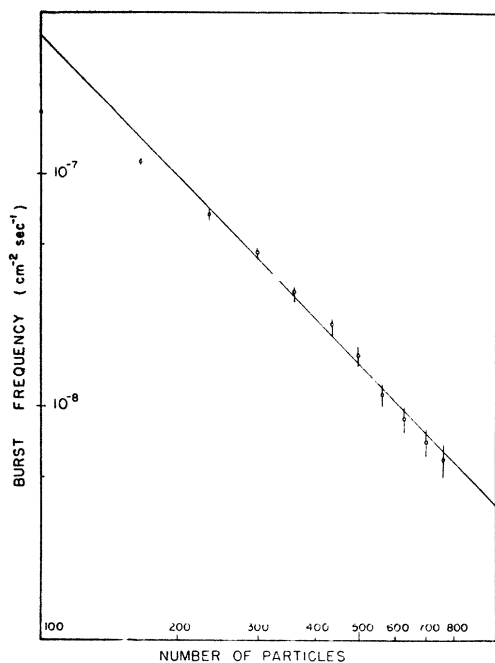


FIG. 11. Integral size-frequency distribution curve for bursts measured under 12 cm of iron at sea level.

power law with exponent $= 2.0 \pm 0.15$, and it is in satisfactory agreement with the value of 1.82 found by Sittkus³⁸ for large bursts measured under a 10-cm iron shield.

The t_0 -, t_m - and t_μ -burst curves which have already been given are compared in Fig. 12. Within the experimental accuracy of these curves, they can all be represented by an integral size-frequency distribution obeying an inverse exponential power law with exponent $= 2.0$. In other words, the three curves corresponding to size-frequency distributions for bursts under 1.25, 12, and 35 cm of iron are nearly parallel; thus integral size-frequency distribution for burst measured under a shield of iron is independent of the thickness of the shield. Since the ratios of the frequencies of the $t_0:t_m:t_\mu$ bursts is independent of burst size, these ratios can be directly evaluated by taking the intercept of each curve with the ordinate in Fig. 12. In this way, $t_0:t_m:t_\mu$ is found to be 1:6.5:2.3 where the t_0 -burst frequency has been taken equal to unity. These values have been used to plot the three-point transition curve given in Fig. 13.

³⁸ A. Sittkus, Zeits. f. Physik 112, 626 (1939).

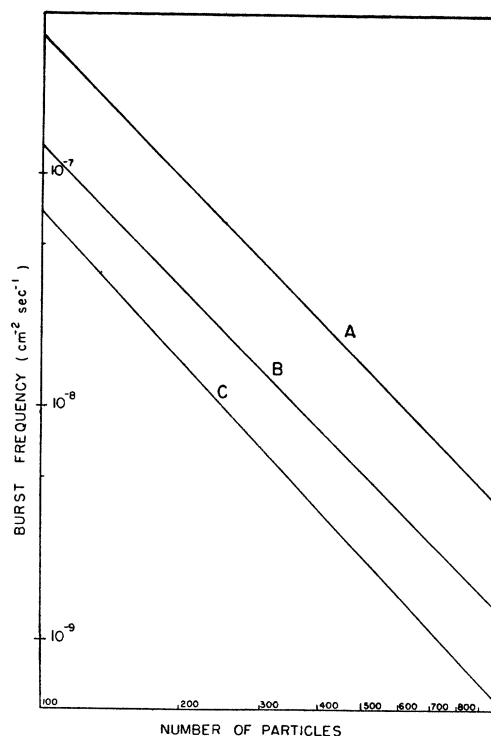


FIG. 12. Comparison of t_0 -, t_m -, and t_μ -burst curves (integral size-frequency distributions). The integral size-frequency distribution curves for bursts measured under 1.25, 12, and 35 cm of iron are given. Curve A is a duplication of Fig. 11, while curve B is redrawn from Fig. 4. Curve C, plotted from the data given in Table III, was given in an earlier publication (see reference 7).

3. Transition Effect

The prohibitive length of time required for obtaining additional data for other intermediate points on the transition curve (Fig. 13) precluded their investigation at this time. In addition, transition curves should be plotted for various

TABLE VI. Integral number of bursts ($\text{cm}^{-2} \text{sec}^{-1}$) with more than S particles produced in 12 cm of iron.

Burst size (in mm)	Burst size (S) (No. of particles)	Integral numbers of bursts (1411 hr.)	Burst frequency ($\text{cm}^{-2} \text{sec}^{-1}$)
1.5- 2.5	100	965	1.84×10^{-7}
2.5- 3.5	167	557	1.12×10^{-8}
3.5- 4.5	234	360	6.85×10^{-8}
4.5- 5.5	300	244	4.65×10^{-8}
5.5- 6.5	367	158	3.02×10^{-8}
6.5- 7.5	434	118	2.25×10^{-8}
7.5- 8.5	500	87	1.66×10^{-8}
8.5- 9.5	567	59	1.12×10^{-8}
9.5-10.5	634	47	8.95×10^{-9}
10.5-11.5	700	37	7.04×10^{-9}
11.5-12.5	767	31	5.92×10^{-9}

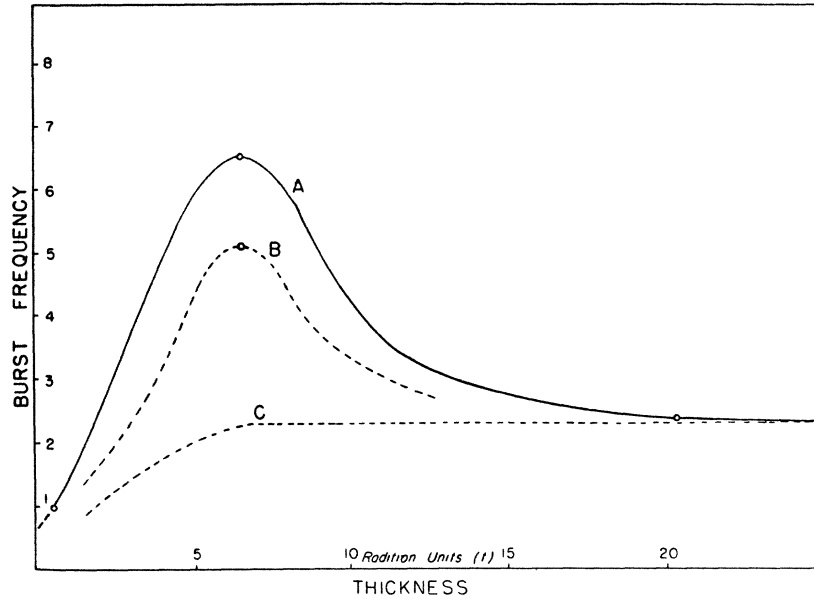


FIG. 13. Analysis of the transition curve for large bursts in iron. From the data given in Fig. 12, the frequency of the bursts observed under 1.25, 12, and 35 cm of iron is plotted as a function of the iron shield thickness as measured in radiation units. The G-M counter coincidence data have been used to effect the decomposition of the transition curve *A* into three components. Thus curve *B* represents the transition effect that would be observed if the effect of extensive air showers was not considered and curve *C* gives the transition expected for bursts originating from knock-on and bremsstrahlung processes in mesotron collisions.

burst size intervals, say from 100 to 300 particles, from 300 to 500, etc. This procedure, if applied to comprehensive burst data covering a wide range of burst size and having high statistical accuracy, could be used to verify the prediction of cascade theory that for the larger burst sizes the maximum in the transition curve should shift to a point corresponding to a greater thickness of shielding material. Such a shift in the maximum cannot be verified from the present experiments because of the lack of sufficient data.

The transition curve given in Fig. 13 exhibits a pronounced maximum. Nie²⁹ also observed a maximum for large bursts at about the same thickness of iron, but the maximum was not as pronounced as that found here. It is believed that this discrepancy can be explained by the fact that the transition curve for large bursts does not represent a simple transition effect involving only one type of cosmic-ray burst. It is, on the contrary, a complex transition and integrates the effect of three burst-producing cosmic-ray components, for each of which the burst frequency is dependent not only upon the geometry of the

chamber and shield but also upon the presence of adjacent dense material. Thus a spherical ionization chamber surrounded by a symmetric shield located in a site free from obstruction by dense material is essential for obtaining interpretable transition curves for large bursts.

Curve *C* is drawn in Fig. 13 to represent the transition effect for bursts produced by knock-on and bremsstrahlung processes of the mesotron. Where the thickness of the chamber shield is greater than 6 or 7 r.u., these t_{μ} -bursts should, in general, be independent of any further increase in this thickness. Thus, at a point on the transition curve corresponding to 12 cm of iron, the contribution to the t_m -burst frequency by bursts produced by mesotrons should be equal to the t_{μ} -burst frequency; this would amount to 35 percent of the t_m -frequency. Since 20 percent of the total t_m -bursts have already been shown to be coincident with extensive showers, there are 45 percent of the t_m -bursts which must be of different origin. Curve *B* (Fig. 13) is sketched to show a possible transition effect for these bursts. It is supposed that these bursts originate from:

- (1) Either the incidence of a very narrow air shower on the ionization chamber.
- (2) Or from single high energy electrons which produce a high multiplication of electrons and photons in the 12 cm of iron.

Supporting the first possibility is the evidence obtained from the coincidence of G-M counter sets with the 20 percent coincident bursts, which shows that many of these bursts are coincident with relatively narrow air showers. Therefore, one could assume that there exist even narrower showers which would not give coincidences with the G-M sets but which would produce bursts under the 12 cm of iron. If these very narrow showers contain a few high energy photons or electrons, these particles would undergo great multiplication in the iron and thus one would not have to postulate high particle densities for these showers. Regarding the second possible origin, it is suggested that single high energy electrons at sea level might arise from the disintegration of short-lived mesotrons. There is, however, no experimental evidence to substantiate this supposition. In order for single electrons to account for the t_m -bursts at sea level, these particles would have to have energies in the range from 10^{10} to 10^{11} ev.

Since for any given thickness of shield less than about 20 r.u., there are three distinct contributions to the observed burst frequency, each of which for a given burst size may have a different total energy associated with it, it is not possible to assign an energy scale to the abscissa of the transition curve. Neither is it possible to select a mono-energetic band of burst producing radiation by merely shielding an ionization chamber with an arbitrary thickness of absorber.

DISCUSSION

The results of the t_0 -, t_m - and t_μ -burst experiments can be summarized in part as follows:

At sea level, the observed cumulative burst frequency $R(t)$ of bursts containing more than 100 particles as observed under a thickness (t) of absorbing shield, is given as:

$$R(t) = R_0(t) + R_x(t) + R_\mu(t), \quad (2)$$

where

$R_0(t)$ is the frequency due to bursts caused by extensive air showers. $R_0(t)$ yields the contribution³⁹ obtained by subtracting curve B from A in Fig. 13.

$R_x(t)$ represents the frequency assumed to be due to either narrow air showers or single high energy electrons. $R_x(t)$ represents³⁹ the difference between curves B and C in the transition curve.

$R_\mu(t)$ is the frequency arising from bursts due to knock-on electrons and bremsstrahlung of mesotrons, as represented by curve C in Fig. 13.

For example, it is seen from Fig. 13 that at a thickness of absorber equal to 7 r.u., $R_0(7)$ contributes approximately 20 percent; $R_x(7)$, 45 percent; and $R_\mu(7)$, 35 percent, respectively, to the observed frequency $R(7)$.

If one excludes burst of origin other than the above three types, then it is obvious that the frequency $R(h, t)$ for any altitude (h) can be given as:

$$R(h, t) = R_0(h, t) + R_x(h, t) + R_\mu(h, t), \quad (3)$$

where the quantities on the right-hand side of the above expression are similar to those defined in Eq. (2), except that they are taken as valid for any altitude (h). Both h and t are measured in r.u. and sea level is defined as $h=0$ r.u.

Since there has been no measurement of the complete transition curve carried out at a higher altitude, say, $h=7$ r.u., one cannot make a thorough comparison of the altitude dependence of the transition curve. However, there have been several experiments performed at higher altitudes from which one can roughly estimate the values for the following ratios:

$$\frac{R(7, 0)}{R(0, 0)} \sim 50 \quad (\text{Kingshill and Lewis}^{34}),$$

$$\frac{R(7, 7)}{R(0, 7)} \sim 15 \quad (\text{Montgomery and Montgomery}^{40}),$$

$$\frac{R(7, 20)}{R(0, 20)} = 4.5 \pm 0.3 \quad (\text{Fig. 9}).$$

Since the ratios $R(0, 0):R(0, 7):R(0, 20)$ have already been given here as 1:6.5:2.3, it can accordingly be estimated that the approximate values of the ratios at altitude $h=7$ r.u. are 50:100:10. These values could be used to indi-

³⁹ This is only approximate since curve B is extrapolated to thicknesses greater than 7 r.u.

⁴⁰ C. G. Montgomery and D. D. Montgomery, Phys. Rev. **47**, 429 (1935).

⁴¹ Actually the value used is $R(0, 0.7)$ but for the present comparison this is approximately $R(0, 0)$.

cate the approximate shape of the transition curve for bursts of more than 100 particles at an altitude of $h=7$ r.u. The fact that the t_μ -burst frequency for such a transition curve is very small compared with the t_0 - and t_m -burst frequencies shows that the great majority of the extensive atmospheric showers at higher altitudes do not contain electrons or photons of energies sufficient to create high multiplication under 20 r.u. (i.e., $E > 10^{11}$ ev).

It is with sincere gratitude that the writer acknowledges the counsel of Professor Marcel Schein who suggested the problem and guided all phases of the investigation. The author is also grateful to Chancellor A. H. Compton for his support and advice. The work was facilitated by a fellowship granted by the Henry Strong Educational Foundation. Appreciation is likewise expressed to the Carnegie Institution of Washington for its cooperation.

Structure in the X-Ray K Absorption Edge of Metallic Potassium

JOSEPH B. PLATT*

Cornell University, Ithaca, New York

(Received December 26, 1945)

For the alkali metals sodium and potassium the free electron approximation should give the energy states in the conduction band closely. Calculations based on this approximation predict an arctangent shape for the potassium K absorption edge. By use of a two-crystal vacuum x-ray spectrometer, the absorption edge of metallic potassium has been explored with high resolving power. Details of the experimental procedure are given. The shape of the absorption edge is in satisfactory agreement with the theoretical arctangent curve, and the width of the edge agrees with the predicted value. Some evidence is found of a secondary structure not given by the simple theory and the free electron approximation. The wave-length of the midpoint of the edge has been redetermined.

INTRODUCTION

RECENT theories of the solid state have predicted the distribution in energy of the conduction electrons in metals. Knowledge of the electronic energy states in the conduction band of a metal makes possible a theory of the structure to be found in the neighborhood of an x-ray absorption edge for that metal, and this derived theory can be tested experimentally. The photoelectric ejection of an electron from the K state of the metal atom, with absorption of the quantum, is permissible if the quantum has sufficient energy to raise the electron to the lowest unoccupied state in the conduction band. Variation of the absorption coefficient for quantum energies starting at this critical value and increasing by a few ev must be due to the nature and density of the energy states in the conduction band.

The experimental requirement is that the absorption coefficient of the metal be investigated carefully over a range of quantum energies of several electron volts including the absorption edge. Since the energy of the absorption edge itself is in general of the order of electron kilovolts, this puts a stringent requirement on the resolving power of the apparatus used. Such resolving power can be obtained without prohibitive loss in x-ray intensity with the two-crystal x-ray spectrometer. A number of investigators have used this research tool to study the structure of absorption edges in metals.^{1,2}

The alkali metals, and especially sodium and potassium, are of particular interest because the theory of their solid state has been developed in some detail. The present study is of the absorption structure in the region of the potassium K

¹ H. Friedman and W. W. Beeman, Phys. Rev. **58**, 400 (1940).

² L. G. Parratt, Phys. Rev. **54**, 99 (1938).

* Now at the University of Rochester.